JOURNAL OF AGRICULTURAL AND FOOD CHEMISTRY
ARTICLE

J. Agric. Food Chem. 2009, 57, 4827–4832 4827
DOI:10.1021/jf9002957

Structural Characteristics of 'Hayward' Kiwifruits from Elephantiasis-Affected Plants Studied by DRIFT, FT-Raman, NMR, and SEM Techniques

Sergio Bonora,*,† Ornella Francioso,‡ Vitaliano Tugnoli,† Antonio Prodi,‡ Michele Di Foggia,† Valeria Righi,† Paola Nipoti,‡ Gianfranco Filippini,‡ and Annamaria Pisi‡

†Dipartimento di Biochimica "G. Moruzzi", University of Bologna, Via Belmeloro 8/2, 40126, Bologna, Italy, and ‡Dipartimento di Scienze e Tecnologie Agroambientali, University of Bologna, Viale Fanin 44, 40127, Bologna, Italy

This is the first study on structural and ultrastructural changes taking place in *Actinidia deliciosa* kiwifruits affected by "elephantiasis syndrome", by means of DRIFT, FT-Raman, NMR, and SEM techniques. The fruits arising from elephantiasis-affected plants assume a round and smaller shape, limiting their marketing. Despite etiological studies on this disease, so far no information is available on the structural and ultrastructural characteristics of the fruits. The SEM and spectroscopic data showed significant modifications regarding the polysaccharide fraction in kiwifruits from diseased plants. The pectins seem to be the polysaccharide fraction more involved in the structural variations of the fruits. These structural and ultrastructural variations are related to the elephantiasis syndrome, and they could be adopted as markers for early diagnosis of the disease.

KEYWORDS: Kiwifruit; elephantiasis; DRIFT; FT-Raman; NMR; SEM

INTRODUCTION

Kiwifruit plants, *Actinidia deliciosa*, are affected by a few biotic diseases responsible mainly for wood damage. Among them, the most destructive and responsible for great yield losses is wood decay, which shows wood with bleached appearance and spongy consistency (*1*). During field investigations for wood decay, we observed an abnormal diametral overgrowth of the trunk in some kiwifruit plants, var. 'Hayward', in orchards in the Emilia-Romagna region (northern Italy). Because of this new finding, etiological and epidemiological studies have been conducted and it has been established that there are two different diseases: wood decay *in sensu strictu* and trunk hypertrophy (*2*). For this last disease Nipoti et al. (*3*) proposed the term elephantiasis, because the huge, abnormal tissue trunk growth resembles an alteration affecting human legs. They found the name elephantiasis to be highly appropriate.

Elephantiasis is characterized by a marked brown area developed from the hypertrophic zone extending to most of the length of the plant, with marked brown discoloration of the annual rings (*4*). The necrotic areas in longitudinal sections of the trunk decrease and appear of cone shape. Elephantiasis can be present at different heights of the trunk, at the collar or at higher portion, so they have been named, respectively, collar and top elephantiasis (*5*). Studies on the etiological and epidemiological aspects of this disease are still in progress and up to now, in plants with elephantiasis, they have shown the presence of a complex mycoflora belonging to the genera *Fusarium* Link ex Fr., *Cylindrocarpon* Wollenw., and *Phialophora*-like taxa (*6*). This similar overgrowth symptom has also been reported in other Italian regions (*6*).

It has also been noted that the fruits arising from elephantiasis-affected plants assume a round and smaller shape, limiting their marketability. Despite studies on the etiological and epidemiological aspects of this disease, to our knowledge, there are no literature data evaluating any metabolic and/or texture alterations of fruits from elephantiasis-affected plants. On the basis of these premises and the primary role of kiwifruit cultivation in the Italian economy (*7*), we have undertaken a study focused on the structure and morphology of kiwifruits from elephantiasis-affected plants using spectroscopic techniques: diffuse reflectance Fourier transform infrared (DRIFT), Fourier transform Raman (FT-Raman), nuclear magnetic resonance (NMR), and scanning electron microscope (SEM).

DRIFT and FT-Raman are complementary spectroscopic methods that have produced useful information on the fruit texture, made of pectin (*8*−*10*), cellulose (*11*), and hemicelluloses (*11*) that influence cell wall polymers. NMR has been used to characterize the chemical composition of juice (*12*, *13*) in kiwifruits.

MATERIALS AND METHODS

Assay for Fruit Characteristics. Five asymptomatic kiwifruit plants and five with elephantiasis were chosen in an orchard in the Veneto region (northen Italy). Ten fruits, from each plant, were randomly harvested and

*Author to whom correspondence should be addressed (telephone 0039 051 2094280; fax 0039 051 243119; e-mail sergio.bonora@unibo.it).

 Published on Web 05/04/2009

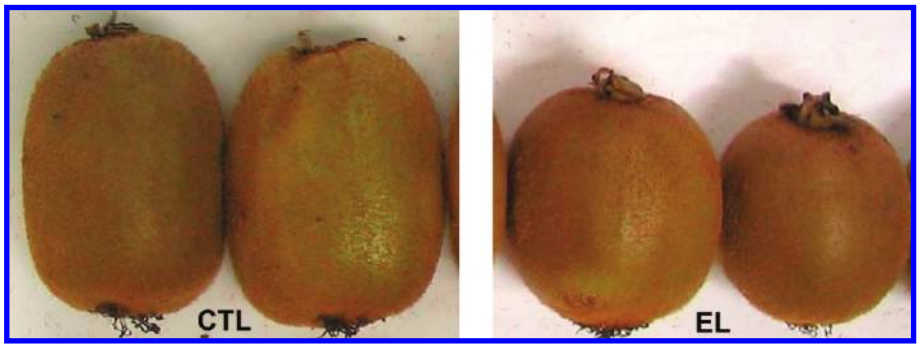

Figure 1. CTL kiwifruits from symptomless plants (left) and EL kiwifruits from elephantiasis-affected plants (right).

designated control fruits (CTL) from symptomless plants and elephantiasis fruits (EL) from elephantiasis-affected plants (**Figure 1**). They were weighed, and their orthogonal diameters were measured (**Figure 2**). Analysis of variance ANOVA was performed using Statgraphics Plus 2.1 software (Statistical Graphics System by Statistical Graphics Corp.). Means were compared according to Tukey's test ($P = 0.05$).

The CTL and EL fruits (total average weight = 1 kg) were washed, and their skins were removed with a lancet. Each fruit was then divided in two parts. One part was cut in thin slices (2−3 mm thick) both for SEM analyses and, after freeze-drying, for FT-Raman measurements. The other part of the fruit was converted into a puree using a mixer and passed through a paddle finisher fitted with seeds to separate the coarse materials. The purees obtained from all of the EL fruits were mixed to obtain a homogeneous sample, freeze-dried, and analyzed by DRIFT and NMR spectroscopies. The same procedure was applied to the CTL fruits.

Scanning Electron Microscopy. Small samples of thin slices (2−3 mm long) from the white part and pulp of CTL and EL kiwifruits were cut, fixed in 5% glutaraldehyde in 0.1 M phosphate buffer, pH 7.2, washed in the same buffer, and dehydrated by passages through graded aqueous ethyl alcohol series (10, 30, 50, 75, 95%). All of the above passages were performed at 5 °C. These specimens were then placed in 100% ethanol at room temperature for a few minutes, dried with a critical point drier unit Balzer CPD 020 (Balzers Union, Ltd., Balzers, Liechtenstein) mounted on aluminum stubs with silver glue, and coated with gold−palladium film using an ion sputtering unit Balzer MED 010 (Balzers Union, Ltd.,). The samples were observed under a scanning electron microscope, Philips 515 SEM (Philips, Eindhoven, The Netherlands) at 7 kV, and pictures were taken with a digital camera Nikon 5400 Coolpix (Nikon, Chiyoda-ku, Tokyo, Japan).

DRIFT Spectroscopy. DRIFT spectra were recorded with a Bruker TENSOR series FT-IR spectrophotometer (Bruker, Ettlingen, Germany) equipped with an apparatus for diffuse reflectance (Spectra-Tech Inc., Stamford, CT). Spectrum was collected as Kubelka−Munk units using KBr (Aldrich Chemical Co. Milwaukee, WI) as background reference. The spectra were collected from 4000 to 400 cm^{-1} and averaged over 100 scans (resolution = 4 cm^{-1}). Analyses of spectroscopic data were performed with Grams/386 spectroscopic software (Galactic Industries, Salem, NH). The second derivatives of the IR spectra were used for wavenumber determination of overlapped bands. The vibrational analyses were performed on the lyophilized kiwifruit puree to avoid water spectroscopic interferences. Standard pectin sample was purchased from Sigma Aldrich (Sigma Aldrich, St. Louis, MO).

Raman Spectroscopy. The FT-Raman spectra were recorded by a Bruker IFS66 spectrometer equipped with a FRA-106 Raman module (Bruker) and a liquid nitrogen cooled Ge-diode detector. The excitation source was an Nd^{3+}-Yag laser (1064 nm) in the backscattering condition, with a laser power of about 100 mW. The spectroscopic resolution was 4 cm^{-1}, and each spectrum was the average of about 15000 scans.

All of the immediately freeze-dried thin fruit slices had separation of the pulp from the white part, and the intermediate region, containing the seeds, was discarded because its presence could disturb the FT-Raman recording.

NMR Spectroscopy. ^{1}H and ^{13}C NMR spectra were recorded at 22 ± 1 °C with a Bruker Avance400 spectrometer (Bruker, Karslruhe, Germany) equipped with a dual $^{1}H/^{13}C$ probe, operating at 400.13 and 100.61 MHz, respectively. NMR spectra were recorded on the lyophilized purees dissolved in deuterated water (D_2O). We used the standard implementations of monodimensional (1D) Bruker NMR experiments. Three different types of 1D proton spectra were acquired by using (a) conventional composite pulse sequence with 1.5 s water-presaturation during relaxation delay, 8 kHz spectroscopic width, 32K data points, and 32 scans; (b) water-suppressed spin−echo Carr−Purcell−Meiboohm−Gill (CPMG) sequence with 1.5 s water presaturation during a relaxation delay of 1 ms echo time and 360 ms total spin−spin relaxation delay, 8 kHz spectroscopic width, 32K data points, and 256 scans; and (c) sequence for diffusion measurements based on stimulated echo and bipolar-gradient pulses with Δ 200 ms, eddy current delay t_e 5 ms, δ 2 × 2 ms, fine shaped gradient with 32 G/cm followed by a 200 μs delay for gradient recovery, 8 kHz spectroscopic width, 8K data points, and 256 scans. Proton-decoupled ^{13}C NMR spectra were accumulated with 32K data points, gated decoupling sequence, 30° pulse angle, 12.8 kHz spectroscopic width, acquisition time of 1.3 s, and a relaxation delay of 2 s. ^{1}H and ^{13}C chemical shifts in D_2O are relative to 3-trimethylsilyltetradeuterosodium propionate (TSP).

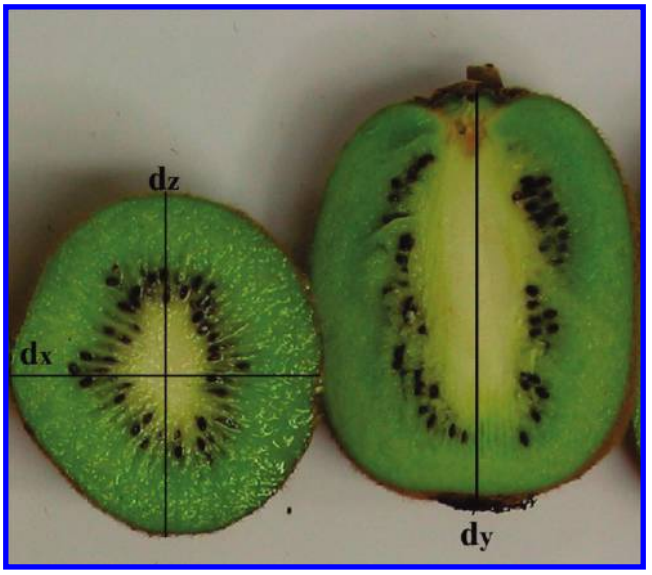

Figure 2. Orthogonal diameters of kiwifruit from symptomless plants.

RESULTS AND DISCUSSION

Average weight and orthogonal diameters of 50 CTL and 50 EL fruits, harvested respectively from five asymptomatic plants and five with elephantiasis, are reported in **Table 1**. All of the data are significantly different ($P = 0.05$). They showed that the EL fruits could be marketed, because their weight (average weight = 98.25 g) is within the commercial standards, but they show alterations in size, especially for d_y, which is 64.88 mm for EL and 68.34 mm for CTL kiwifruits. This parameter influences the typical oval form of kiwifruits of var. 'Hayward', giving a round and almost isodiametric shape to the EL fruits.

Scanning Electron Microscopy. The pulp and the white tissues of the CTL fruits, observed at SEM, showed a well-organized structure and no morphological alterations (**Figure 3A**,**B**). The EL fruit tissue structure was instead degraded, evidencing loss in cell coherence, wall disruption, and collapse (**Figure 3C**,**D**). The SEM data confirm the existence of ultrastructural differences between CTL fruits arising from symptomless plants and EL from elephantiasis-affected plants. It has been demonstrated that during fungal infection there is a wide range of production of pectolytic enzymes (*14*, *15*). The pectin modifications could explain the loss in cell adhesion observed in the EL fruits, taking into consideration the fact that the cellular interfaces, middle lamella, and cell corners are rich in pectins cross-linked by calcium (*16*) and involved in cell adhesion (*17*). Because the fruit texture is made of pectin, cellulose, and hemicelluloses, which mainly depends on the assembly of cell wall (*18*), we can assert that the ultrastructural modifications detectable by SEM indicate a collapse and degradation of cell wall in both the pulp and white part of EL fruits.

Table 1. Average Values of the Weights and Diameters d_x, d_y, and d_z of 10 Fruits from Each of the Five Asymptomatic and Five Elephantiasis-Affected Kiwifruit Plants Tested

fruit	wt (g)	d_x[c] (mm)	d_z[c] (mm)	d_y[c] (mm)
CTL_{1-10}	109.45	52.00	57.30	67.90
CTL_{11-20}	117.15	53.30	57.60	69.80
CTL_{21-30}	101.60	50.70	57.90	68.50
CTL_{31-40}	101.30	48.50	55.70	66.20
CTL_{41-50}	106.10	51.40	56.90	69.30
av CTL[a]	110.52 ± 1.65	51.18 ± 0.36	57.08 ± 0.40	68.34 ± 0.59
EL_{1-10}	114.50	51.10	55.90	68.60
EL_{11-20}	109.45	48.70	56.60	62.10
EL_{21-30}	118.20	51.40	56.60	69.60
EL_{31-40}	97.85	51.00	56.60	65.50
EL_{41-50}	89.85	46.60	52.30	58.60
av EL[a]	98.25 ± 1.79[b]	49.76 ± 0.41	55.60 ± 0.51	64.88 ± 0.77
Fisher's value	25.24^{++}	6.60^{+}	5.17^{+}	12.8^{++}

[a] The average data of CTL and EL fruits from asymptomatic and elephantiasis-affected plants, respectively, are compared according to Tukey's test (P = 0.05). [b] ± Standard error. [c] See **Figure 2**.

DRIFT Spectroscopy. Figure 4 shows the spectra of CTL and EL fruits, pectin standard, and the second derivative. The region between 1800 and 1500 cm^{-1} is of special interest with regard to the evaluation of the degree of esterification, because it allows the observation of infrared absorption of the carboxylic acid and the carboxylic ester groups in pectins (*19*). According to the literature (*9*) the band at around 1740 cm^{-1} corresponds to the absorption of the esterified carboxylic groups of the pectin molecules. In particular, in our samples the maximum of the ester band lies at 1735 cm^{-1} (**Figure 4A**), indicating that the majority of pectins are saturated alkyl esters (*20*). In addition, the bands at 1600 and 1416 cm^{-1}, attributed to the antisymmetric and symmetric $-COO^-$ stretching vibration, respectively, are considered to be diagnostic for the presence of D-galacturonic acid units (*21*). This suggested that a part of the nonesterified carboxylic groups are mostly in the form of carboxylate ions in the kiwifruits. This can be easily seen by observing the pectin spectrum with high degree of esterification (59%) (**Figure 4B**). Proteins might also contribute to the vibrations in the region between 1650 and 1550 cm^{-1}. According to Thygesen et al. (*22*), we assigned the strong bands at about 1640 and 1590 cm^{-1} to amide I and amide II vibrations, respectively, arising from proteins of primary cell wall material. However, it cannot be excluded that the band at 1590 cm^{-1} is due to the aromatic ring stretching (*23*). A weak shoulder at around 1530 cm^{-1} has been assigned to the aromatic system and the double-bond vibrations of ferulate esters attached to neutral sugar side chains of pectins and xylan-type polysaccharides, as also reported by Kacuráková et al. (*21*). The corresponding band was more intense and well resolved in the FT-Raman spectra (**Figure 5**).

The absorbances of the bands at around 1440 and 1330 cm^{-1} are assigned to CH bending modes of pectin methyl ester group and carboxylate symmetric stretching, respectively, and the band at around 1240 cm^{-1} has been assigned to the stretching νCOC of acetyls in acetylated pectates according to the literature (*9*, *11*, *21*). The region between 1100 and 990 cm^{-1} contains skeletal νC−O and νC−C vibration bands of glycosidic bonds and pyranoid

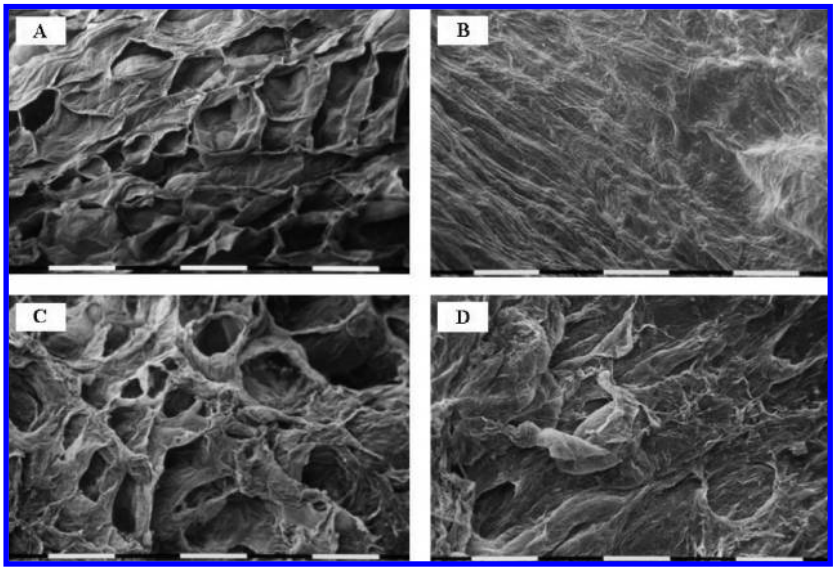

Figure 3. SEM images of the pulp and white part of CTL and EL fruits from symptomless and elephantiasis-affected kiwifruits plants, respectively: (**A**) pulp and (**B**) white part of CTL fruit showing well-organized structure; (**C**) pulp and (**D**) white part of EL fruit showing degradation of the tissue and disrupted cells. Bars = 0.1 mm.

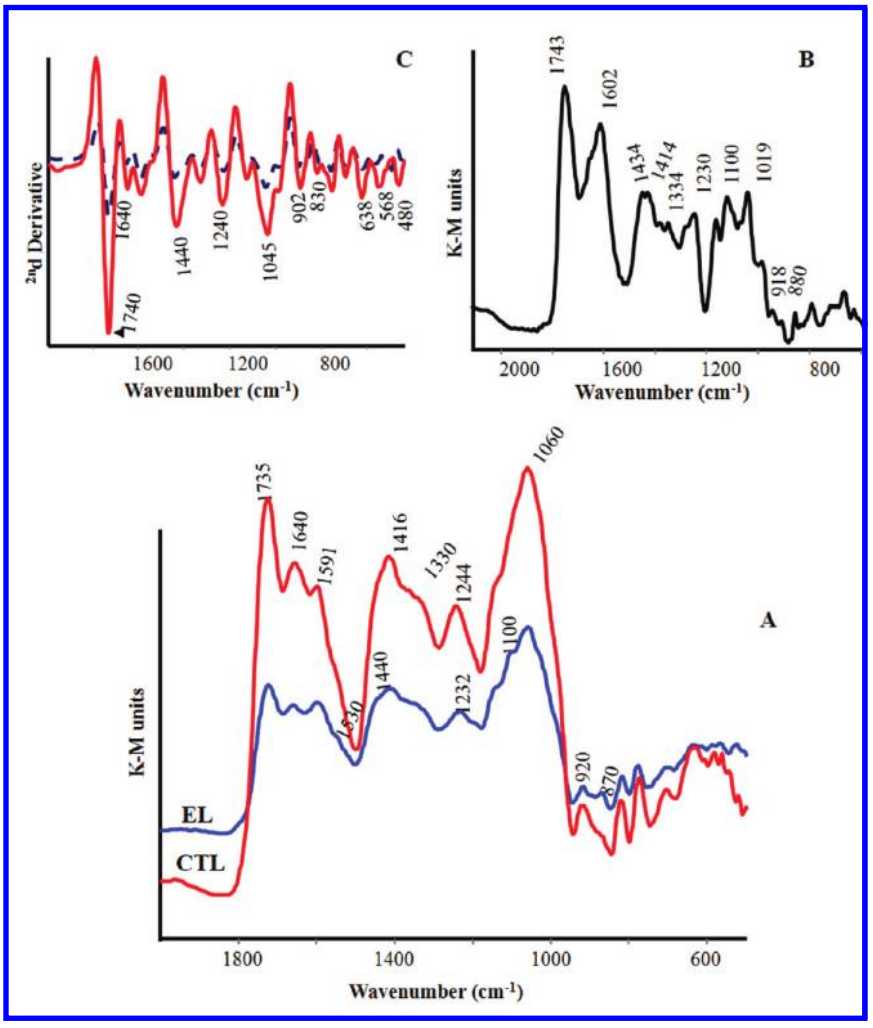

Figure 4. DRIFT spectra of (**A**) CTL and EL kiwifruits from symptomless and elephantiasis-affected plants; (**B**) pectin standard with 59% esterification degree; (**C**) second-derivative of CTL (continuous line) and EL (dotted line) fruits.

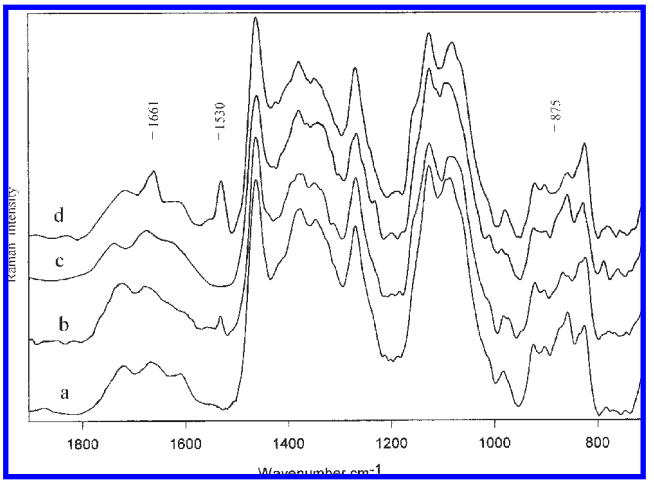

Figure 5. FT-Raman spectra of CTL and EL kiwifruits from symptomless and elephantiasis-affected plants: (**A**) white part and (**B**) pulp of CTL fruits; (**C**) white part and (**D**) pulp of EL fruits.

rings. Moreover, the intense band at 1060 cm^{-1} indicates the presence of hemicellulose, a fruit texture element (*11*).

The bands at around 870 and 920 cm^{-1} are known to be sensitive to the anomeric configuration. These bands were assigned to equatorial anomeric H (α-anomers and α-glycosides) and to axial anomeric H (*β*-anomers and *β*-glycosides), respectively (*24*). In addition, the band at 870 cm^{-1} is also particularly sensitive to the substitution at C6 (*25*). The increased absorbance of the band at 920 cm^{-1} in EL samples (**Figure 4A**) might be associated with the presence of galactose units in accordance with the literature (*11*). On the basis of the enhanced intensity of the band at 920 cm^{-1}, we suppose that there is an increase in free galactose in EL fruits.

The second-derivative analysis (**Figure 4C**) revealed that the spectrum of EL kiwifruits showed a significant decrease in the relative intensity of bands at around 1740 and 1440 cm^{-1} with respect to the same bands of CTL fruits. This change, in accord with previous research (*26*), might suggest a decrease of the degree of esterification of pectins in EL kiwifruits. We also observed a considerable decrease in frequency (−10 cm^{-1}) and intensity of the band at 1240 cm^{-1} in EL fruits, suggesting also a decrease in the acetylation degree. Other structural variations in EL fruits can be observed: (i) decrease of relative intensity of the band at 998 cm^{-1}, assigned to the $\nu O-CH_3$ vibration in methyl esters (*25*, *27*); (ii) disappearance of the band at 830 cm^{-1}, indicating no ester substitution in the C6 position of galacturonic residues; (iii) decrease of band intensity at 638 cm^{-1}, assigned to skeletal bending of pyranose ring; and (iv) disappearance of the band at 568 cm^{-1}, due to the $\nu S-O$ motion in sulfate galactans (*28*). All of these spectroscopic variations are referred to the polysaccharide components.

FT-Raman Spectroscopy. Raman data are complementary to those obtained by DRIFT. **Figure 5** exhibits the spectra in the

1900−750 cm^{-1} spectroscopic region of CTL (**Figure 5A**,**B**) and EL kiwifruits (**Figure 5C**,**D**). In the 4000−1900 cm^{-1} spectroscopic region (data not reported), in which the stretching νC−H modes lie, all spectra are totally overlapping, suggesting that the C−H vibration cannot offer distinguishable aspects between the assayed samples. On the contrary, considering the 1900−750 cm^{-1} spectroscopic region, some characteristic changes can be observed.

The spectra of the pulp of the EL fruits exhibit a considerable increase of the two peaks at 1530 and 1661 cm^{-1} (**Figure 5D**), which are not present or very weak in the CTL fruits as well as in the white part of EL fruits (**Figure 5**). Smaller differences were observed even in the 1000−750 cm^{-1} spectroscopic region; in particular, the peak at about 875 cm^{-1} appears to be less intense in the pulp of the EL fruits (**Figure 5D**), whereas no variation in peak intensity appeared in the spectra of the white part of both EL and CTL fruits.

The peak at 1530 cm^{-1} has been assigned to the C=C bond conjugated with a double bond or with an aromatic ring, and the band at 1661 cm^{-1} is attributed to the stretching vibration of the C=O group conjugate with a double bond as in the ferulate esters (*21*) or in lignin. The existence of different types of phenolic substances, such as ferulic acid derivatives, in plant tissues is a well-known plant response to fungal attack (*29*). We suppose that the strong increase of both 1661 and 1530 cm^{-1} bands in EL pulp spectra is unequivocally related to the infection, and the behavior of these bands might be used as an early marker to evidence fruits arising from diseased plants.

The peak at 875 cm^{-1} could be attributed to the symmetric C−O−C stretching vibration of the ether group, as in the glycosidic bond of the polysaccharides, and is sensitive to substitution at the C6 level (*25*). The reduction of the 875 cm^{-1} peak intensity in the EL fruits confirms pectin degradation as a consequence of fungal infection.

The FT-Raman spectra showed that the chemical modifications are greater in the pulp than in the inner white part of the EL fruits and such a modification takes place in the pectin fraction composition at a level that is not displayed from SEM measurements.

NMR Spectroscopy. Figure 6 reports the comparison of the ^{1}H NMR spectra of CTL (**Figure 6A**,**C**) and EL fruits (**Figure 6B**,**D**). The spectra highlight the presence of narrow and broad resonances, which can be separated using CPMG spin−echo (**Figure 6A**,**B**) and diffusion-edited (**Figure 6C**,**D**) sequences. The narrow resonances arise from low molecular weight metabolites, whereas the diffusion-edited spectrum shows contributions from macromolecules or mobile parts of macromolecules, which are characterized by slow diffusion rate, but not so short to be NMR invisible. It is worth noting that the spectra in **Figure 6A**, **B** and in **Figure 6C**,**D** are practically overlapping, showing a close correspondence with regard to the resonances and their relative intensities. The resonances appearing in the CPMG spectra (**Figure 6A**,**B**) arise mainly from sugars such as α-glucose, β-glucose, fructose, and sucrose (*30*). A signal centered at 2.85 ppm is assigned to citric acid, and a low signal at 4.50 ppm is ascribable to ascorbic acid. The only difference detectable in the diffusion-edited spectra (**Figure 6C**,**D**) is the highest intensity of the resonance at 3.70 ppm in the spectrum of EL fruits. This resonance belongs to glucose-(1→4) units, embedded in small oligosaccharides (*31*). Albersheim and co-workers (*32*) coined the term "oligosaccharin" to describe biologically active oligosaccharides that are produced as a result of the action of either endogenous or microbial enzymes on larger and inactive polysaccharides.

The higher mobility of these oligosaccharides in the EL fruits further confirmed a different structure in accord with the vibrational spectroscopic results. Even the ^{13}C NMR spectra (data not shown) confirm the tight analogy of the molecular composition of CTL and EL fruits.

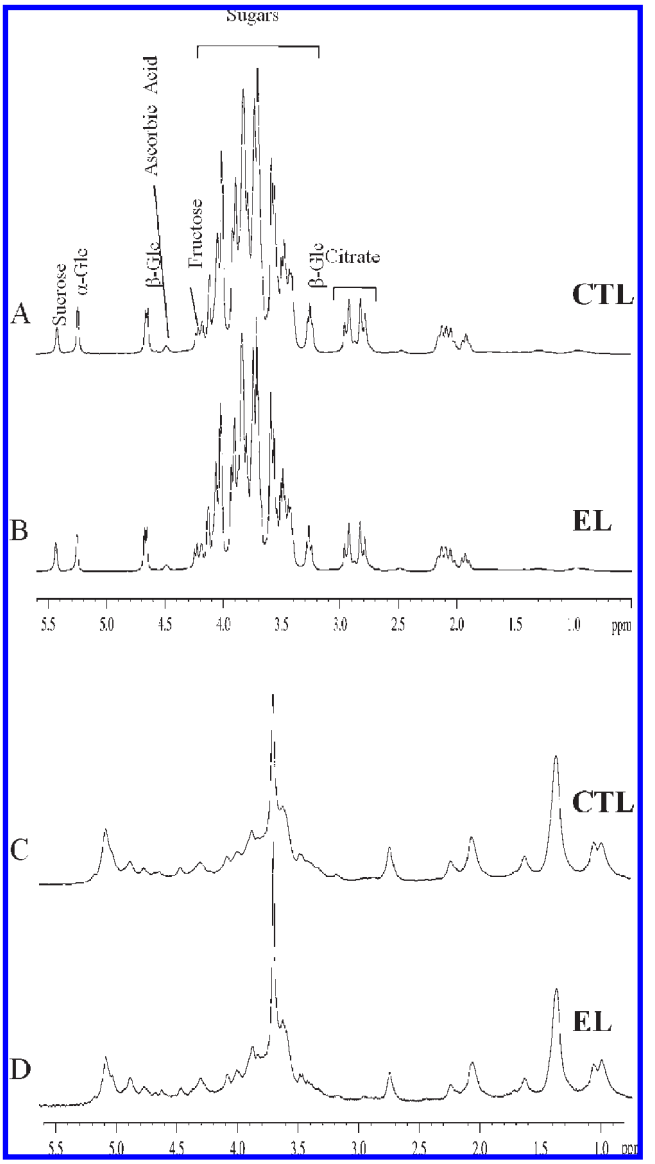

Figure 6. ^{1}H NMR spectra of CTL (**A**, **C**) and EL (**B**, **D**) kiwifruits from symptomless and elephantiasis-affected plants: (**A**, **B**) CPMG; (**C**, **D**) diffusion-edited sequences.

In conclusion, the ultrastructural changes observed at SEM in EL fruits are in accordance with the vibrational spectroscopic data showing that the modifications take place mainly in the polysaccharide fraction. We confirm that pectin esterification degree and the amount of mobile oligosaccharides are a consequence of pathogen infections (*14*, *15*). Therefore, we can assume that these molecules might arise from a discrete degradation process of pectins, probably due to enzymatic activity following fungal infection. Furthermore, the phenolic component is indicative of plant response to fungal attack.

The present study makes a contribution to our understanding of kiwifruit quality related to the elephantiasis syndrome. Studies are in progress to further characterize the chemical modifications occurring in the polysaccharide fraction.

ABBREVIATIONS USED

CPMG, Carr−Purcell−Meiboohm−Gill; DRIFT, diffuse reflectance infrared Fourier transform; FT-Raman, Fourier

transform Raman; NMR, nuclear magnetic resonance; SEM, scanning electron microscope.

ACKNOWLEDGMENT

We thank Dr. Lorenzo Tosi of AGREA srl (S. Giovanni Lupatoto−Verona) and Dr. Tiziano Visigalli of the "Servizio Fitosanitario Regione Veneto" for providing the fruit samples and for field technical help. We also thank Dr. Stefano Tonti for laboratory assistance.

LITERATURE CITED

(1) Calzarano, F.; Spada, G.; Montuschi, C.; Di Marco, S. A new wood decay of kiwifruit in Italy [*Actinidia deliciosa* - Emilia-Romagna]. *Inf. Fitopatol*. **1999**, *49*, 12–15.
(2) Prodi, A.; Sandalo, S.; Nipoti, P.; Credi, R. Molecular identification and characterization of *Phaeoacremonium* spp. isolated from kiwifruit. *J. Plant Pathol*. **2002**, *84*, 191.
(3) Nipoti, P.; Sandalo, S.; Prodi, A.; Credi, R.; Spada, G.; Graziani, S. An unusual wood disease of kiwifruit in Italy. *Acta Hortic*. **2003**, *610*, 253–259.
(4) Nipoti, P.; Prodi, A.; Sandalo, S.; Credi, R. Further study on the main funghi associated with elephantiasis of kiwifruit. *J. Plant Pathol*. **2004**, *86*, 327.
(5) Nipoti, P.; Riccioni, L.; Filippini, G.; Haegi, A.; Prodi, A.; Sandalo, S.; Sequino, S.; Tonti, S.; Valvassori, M. Hypertrophic trunks in Italian kiwifruit orchards. *Proceedings of the 12th Congress of the Mediterranean Phytopathological Union*; Rhodos: Greece, 2006; pp 510−512.
(6) Prodi, A.; Sandalo, S.; Tonti, S.; Nipoti, P.; Pisi, A. Elephantiasis of kiwifruit: characterization of *Phialophora*-like fungi associated with the disease. *J. Plant Pathol*. **2008**, *90*, 487–494.
(7) FAO. FAOSTAT—Statistical Database, FAO Statistics Division, 2008; http://faostat.fao.org/default.aspx (accessed April 10, 2009).
(8) Monsoor, M. A.; Kalapathy, U.; Proctor, A. Improved method for determination of pectin degree of esterification by diffuse reflectance Fourier transform infrared spectroscopy. *J. Agric. Food Chem*. **2001**, *49*, 2756–2760.
(9) Synytsya, A.; Čopíková, J.; Matějka, P.; Machovič, V. Fourier transform Raman and infrared spectroscopy of pectins. *Carbohydr. Polym*. **2003**, *54*, 97–106.
(10) Tamaki, Y.; Konishi, T.; Tako, M. Isolation and characterization of pectin from peel of *Citrus tankan*. *Biosci., Biotechnol., Biochem*. **2008**, *72*, 896–899.
(11) Yashoda, H. M.; Prabha, T. N.; Tharanathan, R. N. Mango ripening-chemical and structural characterization of pectic and hemicellulosic polysaccharides. *Carbohydr. Res*. **2005**, *340*, 1335–1342.
(12) Hills, B. P.; Clark, C. J. Quality assessment of horticultural products by NMR. *Annu. Rep. NMR Spectrosc*. **2003**, *50*, 75–120.
(13) Del Campo, G.; Santos, J. I.; Iturriza, N.; Berrei, I.; Munduate, A. Use of the ^{1}H nuclear magnetic resonance spectra signals from polyphenols and acids for chemometric characterization of cider apple juices. *J. Agric. Food Chem*. **2006**, *54*, 3095–3100.
(14) De Vries, R. P.; Visser, J. *Aspergillus* enzymes involved in degradation of plant cell wall polysaccharides. *Microbiol. Mol. Biol. Rev*. **2001**, *65*, 497–522.
(15) Hunter, J. L.; Thomas, A. G. A.; De Haseth, J. A.; Wickler, L. J. Valencia orange pectinmethylesterase modified pectin characterized by Fourier transform infrared spectroscopy charge fractionation and gelling. *Food Qual*. **2006**, *29*, 479.
(16) Redgwell, R. J.; Fischer, M. Fruit texture, cell wall metabolism and consumer perceptions. In *Fruit Quality and Its Biological Basis*; Knee, M., Ed.; Academic Press: Sheffield, U.K., 2002; pp 1−46.
(17) Jarvis, M. C.; Briggs, S. P. H.; Knox, J. P. Intercellular adhesion and cell separation in plants. *Plant Cell Environ*. **2003**, *26*, 977–989.
(18) Rose, J. C.; Bennett, A. B. Cooperative disassembly of the cellulose-xyloglucan network of plant cell walls: parallels between cell expansion and fruit ripening. *Trends Plant Sci*. **1999**, *4*, 176–183.
(19) Stewart, D.; Morrison, I. M. FT-IR spectroscopy as a tool for the study of biological and chemical treatments of barley straw. *J. Sci. Food Agric*. **1992**, *60*, 431–436.
(20) Parker, F. S. *Application of Infrared, Raman, and Resonance Raman Spectroscopy in Biochemistry*; Plenum Press: New York, 1983.
(21) Kacuráková, M.; Wellner, N.; Ebringerová, A.; Hromádková, Z.; Wilson, R. H.; Belton, P. S. Characterisation of xylan-type polysaccharides and associated cell wall components by FT-IR and FT-Raman spectroscopies. *Food Hydrocolloids* **1999**, *13*, 35–41.
(22) Thygesen, L. G.; Løkkey, M. M.; Micklander, E.; Engelsen, S. B. Vibrational microspectroscopy of food: Raman vs FT-IR. *Trends Food Sci. Technol*. **2003**, *14*, 50–57.
(23) Monsoor, M. A. Effect of drying methods on the functional properties of soy hull pectin. *Carbohydr. Polym*. **2005**, *61*, 362–367.
(24) Cael, J. J.; Koening, J. L.; Blackwell, J. Infrared and raman spectroscopy of carbohydrates. 3. Raman spectra of the polymorphic forms of amylose. *Carbohydr. Res*. **1973**, *29*, 123–134.
(25) Engelsen, S. B.; Nørgaard, L. Comparative vibrational spectroscopy for determination of quality parameters in amidated pectins as evaluated by chemometrics. *Carbohydr. Polym*. **1996**, *30*, 9–24.
(26) Benhamou, N.; Lafontaine, P. J. Ultrastructural and cytochemical characterization of elicitor-induced responses in tomato root tissues infected by *Fusarium oxysporum* f. sp. *radicis-lycopersici*. *Planta* **1995**, *197*, 89–102.
(27) Wellner, N.; Kačuráková, M.; Malovíková, A.; Wilson, R. H.; Belton, P. S. FT-IR study of pectate and pectinate gels formed by divalent cations. *Carbohydr. Res*. **1998**, *308*, 123–131.
(28) Matsuhiro, B. Vibrational spectroscopy of seaweed galactans. *Hydrobiologia* **1996**, *326/327*, 481–489.
(29) Sarma, B. K.; Singh, U. P. Ferulic acid may prevent infection of *Cicer arietinum* by *Sclerotium rolfsii*. *World J. Microbiol. Biotechnol*. **2003**, *19*, 123–127.
(30) Fan, T. V. M.; Lane, A. N. Structure-based profiling of metabolites and isotopomers by NMR. *Prog. Nucl. Magn. Reson. Spectrosc*. **2008**, *52*, 69–117.
(31) Tugnoli, V.; Schenetti, L.; Mucci, A.; Parenti, F.; Cagnoli, R.; Righi, V.; Trinchero, A.; Nocetti, L.; Toraci, C.; Mavilla, L.; Trentini, G.; Zunarelli, E.; Tosi, M. R. *Ex vivo* HR-MAS MRS of human meningiomas: a comparison with *in vivo* ^{1}H NMR spectra. *Int. J. Mol. Med*. **2006**, *18*, 859–869.
(32) Albersheim, P.; Anderson, A. J. Proteins from plant cell walls inhibit polygalacturonases secreted by plant pathogens. *Proc. Natl. Acad. Sci. U.S.A*. **1971**, *68*, 1815–1819.

Received January 26, 2009. Revised Manuscript Received April 21, 2009. This work was supported by grants from Murst (ex 60%) to A. Pisi, S. Bonora, and V. Tugnoli.